DEUTSCHES ELEKTRONEN-SYNCHROTRON **DESY**

DESY 86-099
August 1986

ON THE TOPOLOGICAL STRUCTURE OF SU(2) GAUGE THEORY: A LATTICE INVESTIGATION

by

G. Schierholz

Institut f. Theoretische Physik, Universität Kiel

and

Deutsches Elektronen-Synchrotron DESY, Hamburg

ISSN 0418-9833

NOTKESTRASSE 85 · 2 HAMBURG 52

To be sure that your preprints are promptly included in the HIGH ENERGY PHYSICS INDEX , send them to the following address (if possible by air mail) :

DESY
Bibliothek
Notkestrasse 85
2 Hamburg 52
Germany

DESY 86-099
August 1986

ISSN 0418-9833

On the Topological Structure of SU(2) Gauge Theory: A Lattice Investigation

G. Schierholz

Institut für Theoretische Physik der Universität Kiel
and
Deutsches Elektronen-Synchrotron DESY, Hamburg

Abstract: The lattice formulation and numerical simulations of non-abelian gauge theories enable us to investigate their topological structure in a systematic way. In this talk I shall report on some recent advances in this direction for the pure SU(2) theory, which might serve as a first step towards an understanding of QCD.

Invited talk given at the "International Symposium on Topological and Geometrical Methods in Field Theory", 8-14 June 1986, Espoo, Finland.

1. Introduction

It has been argued since a long time that the (anticipated) dynamical properties of QCD - such as spontaneous chiral symmetry breaking, the solution of the $U_A(1)$ problem, CP conservation and confinement - are, to a large extent, a consequence of the topological structure of the QCD vacuum [1,2]. The key element in this picture is the existence of instantons [3], which carry one unit of topological charge and, owing to the Atiyah-Singer index theorem [4], imply the existence of fermionic zero modes, and which appear to provide a mechanism [2] for regularizing the vortex [5,6] or monopole [7] configurations that have been shown to confine colour.

However, nobody has yet been able to make use of this picture to perform quantitative calculations in continuum, 4-dimensional non-abelian gauge theories. The reason is that instantons have a size parameter ρ, which leads to a divergence at $\rho\to\infty$. At present it is not known how to treat this divergence [8]. Furthermore, for large values of ρ the gauge coupling $g(\rho)$ is not small, and one cannot rely on perturbative results.

The lattice approach to gauge theories, on the other hand, presents a well defined framework in which the static properties of QCD can be calculated explicitly. The main difficulties involved here are in defining and computing the topology of a lattice gauge field configuration and in deriving a more intuitive understanding of the vacuum structure. In the present talk I shall report on recent progress made in this field for the pure SU(2) gauge theory, which I consider to be the first step towards a better understanding of the dynamical properties of QCD.

The talk is organized as follows. In sec. 2 I review the basic elements of topology, emphasizing the points relevant to our lattice calculations. Section 3 contains first results of a quantitative computation of topology and a discussion of the $U_A(1)$ problem. In sec. 4 I report on an attempt to reach an intuitive understanding of the vacuum, and finally in sec. 5 I conclude with some remarks.

2. Topological properties of SU(2) fields

It is not my aim here to give a complete survey of the topological properties of SU(2) gauge fields. Rather, I shall concentrate on those topics, which are of direct relevance to our further discussions, and on some recent developments, which only now have made a solid, quantita-

tive investigation of topology on the lattice feasible.

a. Topological charge

A signal for non-trivial topology is a non-vanishing topological charge [3]

$$Q = -\frac{1}{32\pi^2}\int_M d^4x\, \epsilon_{\mu\nu\rho\sigma}\, Tr\,[F_{\mu\nu}F_{\rho\sigma}] \qquad (1)$$

(M: space-time manifold), which assumes integer values. Geometrically, Q is the second Chern number of the principle bundle underlying the gauge fields.

On the lattice the topological significance of equ. (1) is lost, because naive transcriptions of the integrand are not a total divergence. The topology that we need to study here is that of a principal bundle. Therefore, we cover the (base) manifold M, which for obvious reasons we choose to be a 4-torus, by a set of cells c_i,

$$M \equiv T^4 = \bigcup_i c_i\ , \qquad (2)$$

with $c_{ij} \equiv c_i \cap c_j = \partial c_i \cap \partial c_j$. Since the lattice introduces a cellular structure, it is quite natural to start from this perspective. In each cell c_i we now gauge transform the potentials by

$$A_\mu^{\,i} = g_i^{-1}(A_\mu + \partial_\mu)\, g_i\ , \qquad (3)$$

so that $A_\mu^{(i)}$ is non-singular. On the overlaps c_{ij} the potentials are related by

$$A_\mu^{\,i} = v_{ij}\,(A_\mu^{\,j} + \partial_\mu)\, v_{ij}^{-1}\ , \qquad (4)$$

where

$$v_{ij} = g_i^{-1} g_j\ . \qquad (5)$$

The local sections g_i or, equivalently, the transition functions v_{ij} now completely determine the bundle.

To derive the appropriate expression(s) for the topological charge, we write

$$Q = -\frac{1}{32\pi^2}\sum_i \int_{c_i} d^4x\, \epsilon_{\mu\nu\rho\sigma}\, Tr\,[F_{\mu\nu}^{\,i} F_{\rho\sigma}^{\,i}]\ . \qquad (6)$$

Since

$$-\frac{1}{32\pi^2}\,\epsilon_{\mu\nu\rho\sigma}\, Tr\,[F_{\mu\nu}^{\,i} F_{\rho\sigma}^{\,i}] = \partial_\mu\, \Omega_\mu^{(0)}(i) \qquad (7)$$

with

$$\Omega_\mu^{(0)}(i) = -\frac{1}{8\pi^2}\,\epsilon_{\mu\nu\rho\sigma}\, Tr\,[A_\nu^{\,i}(\partial_\rho A_\sigma^{\,i} + \tfrac{2}{3} A_\rho^{\,i} A_\sigma^{\,i})]\ , \qquad (8)$$

this reduces to

$$Q = \sum_i \int_{\partial c_i} d^3x_\mu\, \Omega_\mu^{(0)}(i) = \sum_{i<j} \int_{c_{ij}} d^3x_\mu\, [\Omega_\mu^{(0)}(i) - \Omega_\mu^{(0)}(j)]\ . \qquad (9)$$

It is elementary to show now that

$$\begin{aligned}\Omega_\mu^{(0)}(i) - \Omega_\mu^{(0)}(j) = \frac{1}{24\pi^2}\,\epsilon_{\mu\nu\rho\sigma}\,\{ & Tr\,[g_i^{-1}\partial_\nu g_i\, g_i^{-1}\partial_\rho g_i\, g_i^{-1}\partial_\sigma g_i] - (i\to j) \\ & - 3\,\partial_\nu\, Tr\,[\partial_\rho g_i\, g_i^{-1}\partial_\sigma g_i\, g_i^{-1}]\,\} \qquad (10)\\ = -\frac{1}{24\pi^2}\,\epsilon_{\mu\nu\rho\sigma}\,\{ & Tr\,[v_{ij}^{-1}\partial_\nu v_{ij}\, v_{ij}^{-1}\partial_\rho v_{ij}\, v_{ij}^{-1}\partial_\sigma v_{ij}] \\ & - 3\,\partial_\nu\, Tr\,[\partial_\rho v_{ij}\, v_{ij}^{-1} A_\sigma^{\,i}]\,\}\ ,\end{aligned}$$

which finally leads to expressions

$$Q = \frac{1}{24\pi^2}\sum_i \int_{\partial c_i} d^3x_\mu\, \epsilon_{\mu\nu\rho\sigma}\, Tr\,[g_i^{-1}\partial_\nu g_i\, g_i^{-1}\partial_\rho g_i\, g_i^{-1}\partial_\sigma g_i] \qquad (11)$$

and

$$\begin{aligned} Q = & -\frac{1}{8\pi^2}\sum_{i<j<k} \int_{c_{ijk}} d^2x_{\mu\nu}\, \epsilon_{\mu\nu\rho\sigma}\, Tr\,[v_{ij}^{-1}\partial_\rho v_{ij}\, v_{kj}^{-1}\partial_\sigma v_{kj}] \qquad (12)\\ & -\frac{1}{24\pi^2}\sum_{i<j} \int_{c_{ij}} d^3x_\mu\, \epsilon_{\mu\nu\rho\sigma}\, Tr\,[v_{ij}^{-1}\partial_\nu v_{ij}\, v_{ij}^{-1}\partial_\rho v_{ij}\, v_{ij}^{-1}\partial_\sigma v_{ij}]\end{aligned}$$

($c_{ijk} = c_i \cap c_j \cap c_k$), respectively, which only involve the local sections or transition functions.

Expression (12) was first derived by Lüscher [9]. In ref. [10] it was then shown that in SU(2) one can use the cochain reduction [11] to integrate equ. (12) completely:

$$Q = Q^{(1)} + Q^{(2)} + Q^{(3)} + Q_\Sigma^{(3)}\ . \qquad (13)$$

Each term is a sum of integers

$$Q^{(i)} = \sum n^{(i)}, \; i = 1,2,3, \qquad Q^{(3)}_{\Sigma} = \sum n \;, \tag{14}$$

where n is the winding number associated with lattice points $c_i \cap c_j \cap c_k \cap c_l \cap c_m$ and $n^{(1)}$, $n^{(2)}$ and $n^{(3)}$ arise from gauge singularities along faces, plaquettes and links of the cells, respectively.

It is also possible to integrate equ. (11), because again the integrand is (almost everywhere) a total divergence. Writing

$$g_i = \exp(i\vec{\alpha}\vec{\tau}) = \cos\alpha + i\vec{e}_\alpha\vec{\tau}\sin\alpha, \tag{15}$$

one finds that the only contribution to Q comes from "vortices" at which $g_i = -1$, i.e. $\alpha = \pi$ [10,11,12]:

$$Q = Q^{(1)} = \sum n^{(1)}(x_s; i) \tag{16}$$

with

$$n^{(1)}(x_s;i) = \frac{1}{8\pi^2} \int_{S^2_\varepsilon(x_s)} d^2x_{\mu\nu}\, \epsilon_{\mu\nu\rho\sigma}\, \vec{e}_\alpha \cdot (\partial_\rho \vec{e}_\alpha \times \partial_\sigma \vec{e}_\alpha) \in \mathbb{Z}, \tag{17}$$

where $S^2_\varepsilon(x_s)$ is a sphere of radius ε around the location $x_s \in \partial c_i$ of the vortex with orientation induced from ∂c_i. Computationally, equ. (16) shows special promise since it only requires to locate the (gauge) singularities of the local section.

To define a smooth bundle to a lattice gauge field configuration requires interpolation from the lattice points to any point in ∂c_i. An efficient procedure would be to extend the lattice gauge fields to the bundle such that the image of ∂c_i under the map g_i decomposes into spherical polyhedra. Then the search for singularities x_s reduces to the computation of at most 4x4 determinants. Such an interpolation exists now for SU(2) [13]. As the cells discussed above these authors consider the dual cells surrounding the sites of a simplicial lattice. To exploit this algorithm on a usual hypercubic lattice one must slice a hypercube into simplices.

b. Zero modes

A further, though related, signal for topologically non-trivial properties of the gauge fields is the occurrence of zero modes in the spectrum of the euclidian Dirac operator.

The point of contact between the fermionic and bosonic sectors of

the theory is the Atiyah-Singer index theorem [4], which relates the number of right-handed (n_+) and left-handed (n_-) normalizable zero modes to the topological charge by

$$n_+ - n_- = Q. \tag{18}$$

A similar theorem in 3 space-time dimensions has been proved by Callias [14]:

$$n_+ - n_- = q, \tag{19}$$

where q is the magnetic charge.

To expose the index theorem and its physical consequences on the lattice, one has to make a choice of fermions. There are several ways of putting fermions on a lattice. None of them is entirely satisfactory in preserving the continuum symmetries. For our purposes Kogut-Susskind fermions [15] are best suited, since they have simpler chiral properties than other fermions. Their action is

$$\begin{aligned} S_F &\equiv \bar{\chi}\,[M + 2ma]\,\chi \\ &= a^3 \sum_x \Big[\sum_\mu (\bar{\chi}_x (-1)^{\hat{x}_1 + \cdots + \hat{x}_{\mu-1}} U_{x,\mu}\, \chi_{x+\hat{\mu}} - \text{h.c.}) + 2ma\, \bar{\chi}_x \chi_x \Big], \end{aligned} \tag{20}$$

where $U_{x,\mu}$ is the link matrix,

$$U_{x,\mu} = \exp\Big(i \int_x^{x+\hat{\mu}} dx_\mu A_\mu\Big), \tag{21}$$

and a the lattice spacing, and where $\bar{\chi}_x$, χ_x are single-component (coloured) Grassmann fields defined at the lattice point x, which on a hypercube combine to define 4 flavours of Dirac fermions. Alternatively, Kogut-Susskind fermions may be viewed as a lattice version of the Dirac-Kähler equation [16].

There are no exact zero modes for Kogut-Susskind fermions. But there are "approximate" zero modes, whose eigenvalues will become exactly zero in the continuum limit a→0, and they will have anomalies appropriate to 4 flavours [17]:

$$n_+ - n_- = 4Q. \tag{22}$$

To test and exploit equ. (22) (on the lattice) in full detail, we will have to identify the appropriate currents and the γ_5 operator. Work along these lines is in progress. If one is only interested in the existence (or non-existence) of zero modes or in their total number, it is sufficient to diagonalize M [18]: the number of zero modes (and approximate zero modes for finite a, respectively) of M, $\#_0(M)$, is

$$\#_0(M) = n_+ + n_- . \qquad (23)$$

In 3 space-time dimensions the same results apply with Q replaced by q.

Semi-classically, n_+ counts the number of instantons (monopoles) and n_- the number of antiinstantons (antimonopoles).

c. Physical consequences

The physical consequences of gauge field configurations with non-trivial topology enter through the anomaly

$$\int_M d^4x \, \frac{1}{2} \partial_\mu J^5_\mu = n_+ - n_- = Q . \qquad (24)$$

The anomaly breaks the classical $U_A(1)$ invariance of the QCD Lagrangian, so that Goldstone's theorem is evaded, and there need not be a nearly massless meson with the quantum numbers of the η'. Indeed, it turns out that the mass of the η' is related to the topological susceptibility

$$\chi_t = \langle Q^2 \rangle / V \qquad (25)$$

(V: volume of space-time manifold M) by [19]

$$m_{\eta'}^2 + m_\eta^2 - 2m_K^2 = \frac{2N_f}{f_\pi^2} \chi_t \qquad (26)$$

as the number of colours $N_c \to \infty$. Owing to the qualitative success of large N_c predictions, we anticipate that (using N_f = 3 light flavours)

$$\chi_t \approx (180\ \mathrm{MeV})^4 . \qquad (27)$$

As a further consequence topological non-triviality may cause spontaneous chiral symmetry breaking. The latter has been studied on the lattice [20]. For the order parameter one finds

$$\langle \bar\psi \psi(m) \rangle = \frac{a}{V} \langle \mathrm{Tr} [M + 2ma]^{-1} \rangle = \frac{a}{V} \left\langle \sum_i \frac{ma}{\lambda_i^2 + (2ma)^2} \right\rangle$$

$$\xrightarrow[V \to \infty]{} N_c a^{-3} \int_{-\infty}^{+\infty} d\lambda \, \frac{ma \, \rho(\lambda)}{\lambda^2 + (2ma)^2} , \qquad (28)$$

where $\{\lambda_i\}$ are the eigenvalues of M, and

$$\lim_{m \to 0} \lim_{V \to \infty} \langle \bar\psi \psi(m) \rangle = N_c a^{-3} \pi \rho(0) . \qquad (29)$$

Thus, spontaneous chiral symmetry breaking requires the occurrence of zero modes. But they do not need necessarily be normalizable [21].

Other, more speculative ideas about the involvement of topology in the dynamics of QCD will be touched upon later.

3. Towards a quantitative study of topology: the $U_A(1)$ problem

So far the only quantity showing clear proof of non-trivial topology that one has been able to calculate quantitatively is the topological susceptibility χ_t, which plays a key role in the resolution of the $U_A(1)$ problem [equs. (24)-(27)].

The calculation of χ_t involves to generate equilibrium gauge field configurations and to compute their topological charge Q. To make contact to the η' mass through equ. (26), which holds in the large N_c limit, the gauge field configurations are to be generated in the pure gauge theory.

In table 1 and fig. 1 I have summarized the results of a recent high statistics calculation [12,22] of χ_t based on the fast algorithm described in sec. 2a. Further details of the calculation and a comparison to previous work on smaller lattices [23] can be found in the original papers. Table 1 indicates that finite volume effects are quite likely small for the $V=10^4$, $\beta=2.3$ and $\beta=2.4$ and $V=12^4$, $\beta=2.5$ simulations. The curve in fig. 1 represents the fourth power of the 2-loop renormalization group formula for the lattice spacing a,

$$a = \Lambda_L^{-1} \left(\frac{6}{11} \pi^2 \beta \right)^{\frac{51}{121}} \exp\left(-\frac{3}{11} \pi^2 \beta \right) \qquad (30)$$

normalized to $a^4 \chi_t$ at $V = 10^4$, $\beta = 2.4$. We notice that $a^4 \chi_t$ does not scale asymptotically (yet). But, using the results of ref. [24], we find that the topological susceptibility shows the same deviations from asymptotic scaling (or better: displays the same β-function) as the string tension K, which gives us confidence that we see continuum physics.

To compute the topological susceptibility in physical units, we need to set the scale. The string tension calculation [24] gives, assuming $\sqrt{K}$ = 400 MeV, Λ_L = 6.6 MeV. Using the $V = 10^4$, $\beta = 2.4$ result one then obtains

$$\chi_t = (262 \pm 1\ MeV)^4 . \qquad (31)$$

This is not in quantitative agreement with equ. (27). However, considering the limitations of the large N_c expansion, the agreement is quite satisfactory.

4. Rudiments of an intuitive understanding of the topology of the vacuum

In the above no reference is made to instantons. They play a role in the semi-classical analysis of the problem and offer an intuitive understanding of topology, but until a year ago it was not certain whether they existed in the quantum vacuum or not.

The way to find out [25,26,27] whether there are instantons, or any other semi-classical objects, underlying the vacuum is to start from an equilibrium gauge field configuration and freeze their quantum fluctuations by an appropriate relaxation procedure. If instantons exist, they should remain behind and become clearly visible, as they are solutions of the classical equations of motion and, hence, are stable under relaxations. On the lattice they are, of course, only quasi-stable.

To be specific, one generates equilibrium SU(2) gauge field configurations using (e.g.) Wilson's action

$$S = \beta \sum_{x \atop \mu<\nu} (1 - \tfrac{1}{2} Tr\, U_{x,\mu\nu}) = \beta \sum_{x \atop \mu<\nu} [1 - \tfrac{1}{2} Tr (U_{x,\mu} U_{x+\hat{\mu},\nu} U^{+}_{x+\hat{\nu},\mu} U_{x,\nu})] . \qquad (32)$$

One then replaces successively each link matrix by

$$U_{x,\mu} \to U^{new}_{x,\mu} = c \sum_{\nu>\mu} [U_{x,\nu} U_{x+\hat{\nu},\mu} U^{+}_{x+\hat{\mu},\nu} + U^{+}_{x-\hat{\nu},\nu} U_{x-\hat{\nu},\mu} U_{x+\hat{\mu}-\hat{\nu},\nu}] , \qquad (33)$$

where c is a normalization constant such that $U^{new}_{x,\mu} \in SU(2)$, which leaves us after a number of sweeps through the lattice with solutions of the classical lattice field equations

$$\frac{\delta S}{\delta U_{x,\mu}} = 0 . \qquad (34)$$

a. Zero temperature [25]

Let me first discuss now what evidence for an underlying semi-classical structure there is in the zero temperature phase, i.e. in the ordinary vacuum, which is supposed to confine.

Figure 2 shows the history of 4 typical gauge field configurations, which where generated at $\beta = 2.1$ on a 6^4 lattice in the pure gauge theory, as a function of the number of relaxation sweeps through the lattice. While configuration A decays into the trivial vacuum, configurations B,C and D show plateaus at

$$S \approx \beta\, 2\pi^2 N , \quad N = 1, 2, \cdots , \qquad (35)$$

which indicate the existence of quasi-stable solutions of the classical field equations. This is precisely what one expects for an underlying (multi-) instanton field configuration.

To prove that these objects are really instantons, one has to show that their action density is localized in space-time, that they have the appropriate topological charge and that they give rise to zero modes in accord with the index theorem (18). In fig. 3 I have plotted the action density

$$S_x = \tfrac{1}{6} \beta \sum_{\mu<\nu} (1 - \tfrac{1}{2} Tr\, U_{x,\mu\nu}) \qquad (36)$$

in units [100 S_x/β] for a 3-dimensional cross section through the center of the would-be instanton of configuration B (after 30 sweeps). This and similar plots for configurations C and D indicate that the action is indeed concentrated in small space-time regions. To prove that also the two other requirements are satisfied, I have plotted in fig. 4 the history of another 3 typical configurations, this time generated at β=2.2 (for a change). Also shown is the eigenvalue spectrum of M and the topological charge Q, which were computed at the positions marked by arrows. Configuration E, which decays to the trivial vacuum, has Q=0 and no (approximate) zero mode. Configuration F(G), which has action N=1 (N=2) and Q=+1 (Q=+2) and consequently is self-dual, has 1(2) zero modes (which is hard to recognize in fig. 4), not counting the fourfold degeneracy due to fermion doubling. So, we may say that we see instantons.

Meanwhile, this kind of investigation has been repeated on larger lattices and for larger values of β [28] (and even including dynamical fermions [29]). The result is much the same. It seems though that the vacuum is more complicated than being simply a dilute gas of instantons and antiinstantons [22]. In this context I also like to mention that, relying on these methods, it is hard to distinguish an instanton from a not too widely separated meron [2] pair: presumably, the relaxation procedure will drive the meron pair to an instanton. Moreover, it is conceivable that a widely separated meron pair will decay rather quickly.

b. Finite temperature [30]

To complete the picture of the vacuum, it is useful to study it at finite temperature: as the time dimension of the lattice is made smaller, fluctuations with large scale size which are responsible for confinement will eventually break down to their more elementary "constituents". Furthermore, the finite temperature deconfined phase of QCD has long attracted interest as a novel form of matter [31], but very little is known about its physics [32].

Before I shall present some recent work going in this direction, let me first remind you of the global properties of the finite temperature vacuum [33]. For high temperatures the functional integral is highly peaked about configurations, which are static up to a gauge transformation. This implies that

$$E_i^2(x) = a^{-2}(1-\tfrac{1}{2}\mathrm{Tr}\,U_{x,0i}) \underset{T\to\infty}{=} 0 \qquad (37)$$

and

$$L(x) = \tfrac{1}{2}\mathrm{Tr}\prod_n U_{x+n\hat{0},0} \in Z_2 = \{\pm 1\}, \qquad (38)$$

where E is the colour electric field, L the Wilson line and T the temperature. The fact that $L(x)\neq 0$, i.e. that the center symmetry is spontaneously broken, establishes the existence of a high-temperature non-confining phase. A further consequence is that the dynamics of the spatial degrees of freedom is essentially that of the corresponding zero temperature theory in 3 space-time dimensions.

To investigate the structure of the finite temperature vacuum, one proceeds exactly as before: generate equilibrium gauge field configurations at the desired temperature, freeze the quantum fluctuations (slowly) and see what is left behind. In fig. 5 I have plotted the results for a selection of typical configurations, which were generated at $\beta=2.4$ on a $10^3\cdot 4$ lattice. This corresponds to a temperature well above the deconfinement phase transition. Configuration H decays to the trivial vacuum. Configuration I shows a plateau about $s=\beta 2\pi^2$, which suggests that this carries an instanton or antiinstanton. Calculations of the topological charge and the zero modes prove that this is indeed the case. Most interesting and indicating new physics are configurations J and K. Configuration J shows a plateau about half the height of that of an instanton. On the plateau one finds Q=0, and the (4-dimensional) Dirac operator has no zero mode. Configuration K shows a hint

of a plateau about $S/8 \approx 30$. On the first "plateau" one finds Q=1 and one zero mode, while the second plateau has Q=0 and no zero mode as in configuration J. This indicates that configuration K contains an instanton plus the object seen in configuration J.

To illuminate what these objects are, I have plotted in fig. 6 the colour electric and colour magnetic field strengths separately. One sees that on the plateau

$$\vec{E}^2(x) \simeq 0. \qquad (39)$$

Further calculation of the Wilson line on the plateaus gives

$$L(x) \simeq \pm 1. \qquad (40)$$

(It is not known yet whether the two values (±1) balance or not.) Equations (39) and (40) mean that these objects are static (approximate) solutions of the classical equations of motion. Indeed, if one computes the action density, one finds this to be exactly the same for all time slices. Furthermore, one finds that the action is localized. In fig. 7 I have plotted the density

$$D_x = \tfrac{1}{3}\beta\sum_{i<j}(1-\tfrac{1}{2}\mathrm{Tr}\,U_{x,ij}) \equiv \tfrac{1}{3}\beta a^2\vec{B}(x)^2, \qquad (41)$$

where B is the colour magnetic field, in units $[10D_x/\beta]$ for a 2-dimensional cross section through the center. It is striking though that the action density falls off much slower than in case of the instanton (fig. 3).

A further striking property of this object is the value of its action, which is about half of that of an instanton. To demonstrate that this is indeed a genuine property, I show in fig. 8 a comparison of results on $8^3\cdot 4$, $10^3\cdot 4$ and $12^3\cdot 4$ lattices, which all point at the same value.

What is the origin of these field configurations now? A solution of the equations of motion of exactly the kind we have found is the well-known Wu-Yang monopole [34]

$$B_i^a(x) = \frac{x_i x_a}{r^4}, \quad r^2 = \vec{x}^2,$$
$$E_i^a(x) = 0 \qquad (42)$$

(a: colour index), which suggest that they are monopoles. The only drawback is that the Wu-Yang monopoles have an infinite action and so must

be smoothed at the origin to qualify as a candidate. A monopole carries one unit of magnetic charge. To show that this is also the case for our solution, I have calculated the magnetic charge by computing the total magnetic flux out of a surface enclosing the "monopole" [35] (with Ao playing the role of the Higgs field). The result pointed at the right value but was not totally unambiguous because of the size of the "monopole" and the relatively small lattice [cf. fig. 7], and I therefore will not report it here. Instead, I will present another proof, which employs the Callias index theorem (19). In fig. 9 I have plotted the eigenvalue spectrum of the 3-dimensional (spatial) analogue of the fermion matrix M [equ. (20)], i.e. the eigenvalues of the 3-dimensional Dirac operator. (That makes sense, because the field configurations under consideration are static up to gauge transformations.) The spectrum in fig. 9a corresponds to configuration H [cf. fig. 5] (after 20 sweeps), which has decayed to the trivial vacuum. One finds no zero mode. The spectrum in fig. 9b corresponds to configuration J (after 20 sweeps), which has a plateau about half the height of that of an instanton. In this case one finds one zero mode (modulo the flavour degeneracy). According to the index theorem (19), one zero mode implies one unit of magnetic charge. This completes the proof: what we have found are indeed monopoles. A further study shows that monopoles are the dominant underlying field configurations in the deconfinement phase [30], while in the confinement phase we mostly find instantons [30,36].

This is as far as we have got in our intuitive understanding of the vacuum. If we could work these results - instantons in the confined phase and monopoles in the high-temperature, deconfined phase - into a coherent picture, we would have a model for confinement. The fact that the monopoles have about half the action of an instanton suggests that they descend from merons (remember: 3-dimensional cross sections of merons are monopoles), which can be viewed as constituents of instantons [2].

5. Outlook

One may say that - thanks to the lattice approach - topological research in gauge theories has entered a new stage: solid computations of topology are now possible, and one can eventually test which of the various confinement schemes discussed in the literature is realized in nature.

One would like to extend these calculations to the physically more

interesting gauge group SU(3) and to include dynamical fermions. In principle this is possible. A first attempt to compute χ_t for SU(3) has been made in ref. [37]. This calculation required, however, a major commitment of computer time and therefore was restricted to small lattices, since for the SU(3) topological charge there is no fast combinatoric algorithm yet. A breakthrough in this direction is badly needed. As far as dynamical fermions are concerned, the interrelation of topology and the essentially zero light quark masses require an exact updating procedure. Such a procedure exists [38], but it is very time consuming too.

References

1) G. 't Hooft, Phys. Rev. Lett. 37, 8 (1976); Phys. Rev. D14, 3432 (1976).

2) C. Callan, R. Dashen and D. Gross, Phys. Rev. D17, 2717 (1978).

3) A.A. Belavin, A.M. Polykov, A.S. Schwartz and Yu. S. Tyupkin, Phys. Lett. 59B, 85 (1975).

4) M. Atiyah and I. Singer, Ann. Math. 87, 484 (1968).

5) G. 't Hooft, Nucl. Phys. B138, 1 (1978); B153, 141 (1979).

6) G. Mack, in Recent Developments in Gauge Theories, ed. G. 't Hooft et al. (Plenum, New York, 1980).

7) S. Mandelstam, Phys. Rep. 23C, 245 (1976).

8) B. Berg and M. Lüscher, Nucl. Phys. B160, 281 (1979), have solved this problem for the CP^{N-1} model. But there is no agreement on the implications of the results on QCD.

9) M. Lüscher, Comm. Math. Phys. 85, 29 (1982).

10) M. Göckeler, M.L. Laursen, G. Schierholz and U.-J. Wiese, DESY report 85-142 (1985), to appear in Comm. Math. Phys.

11) M.L. Laursen, G. Schierholz and U.-J. Wiese, Comm. Math. Phys. 103, 693 (1986).

12) A.S. Kronfeld, M.L. Laursen, G. Schierholz and U.-J. Wiese, DESY report 86-082 (1986).

13) A. Phillips and D. Stone, Comm. Math. Phys. 103, 599 (1986).

14) C. Callias, Comm. Math. Phys. 62, 213 (1978).

15) J. Kogut and L. Susskind, Phys. Rev. D11, 395 (1975); L. Susskind, Phys. Rev. D16, 303 (1977).

16) P. Becher and H. Joos, Z. Phys. C15, 343 (1982).

17) M. Stone, Ann. Phys. 155, 56 (1984).

18) I. Barbour, N.-E. Behilil, P. Gibbs, G. Schierholz and M. Teper, in The Recursion Methods and its Applications, eds. D. Pettifor and D. Wearie, Solid State Sciences 58 (Springer, Berlin, Heidelberg, New York, Tokyo, 1985).

19) E. Witten, Nucl. Phys. B156, 269 (1976); G. Veneziano, Nucl. Phys. B159, 213 (1979).

20) I. Barbour, P. Gibbs, J.P. Gilchrist, G. Schierholz, H. Schneider and M. Teper, Phys. Lett. 136B, 80 (1984).

21) E. Floratos and J. Stern, Phys. Lett. 119B, 419 (1982).

22) A.S. Kronfeld, M.L. Laursen, G. Schierholz, C. Schleiermacher and U.-J. Wiese, DESY report to be published.

23) I.A. Fox, J.P. Gilchrist, M.L. Laursen and G. Schierholz, Phys. Rev. Lett. 54, 749 81985); Y. Arian and P. Woit, Nucl. Phys. B268, 521 (1986); G. Lasher, A. Phillips and D. Stone, in Quark Confinement and Liberation: Numerical Results and Theory, eds. F. Klinkhammer and M.B. Halpern (World Scientific, Singapore, 1985).

24) F. Gutbrod and I. Montvay, Phys. Lett. 136B, 411 (1984).

25) E.-M. Ilgenfritz, M.L. Laursen, M. Müller-Preußker, G. Schierholz and H. Schiller, Nucl. Phys. B268, 693 (1986).

26) M. Teper, Phys. Lett. 162B, 357 (1985).

27) A similar procedure has been previously applied to the O(3) sigma model by B. Berg, Phys. Lett. 104B, 475 (1981); Y. Iwasaki and T. Yoshié, Phys. Lett. 127B, 197 (1983).

28) M.L. Laursen and G. Schierholz, unpublished.

29) I. Barbour, P. Gibbs and G. Schierholz, unpublished.

30) M.L. Laursen and G. Schierholz, DESY report in preparation.

31) K. Kajantie (ed.), Quark Matter '84, Lecture Notes in Physics (Springer, Berlin, Heidelberg, New York, Tokyo, 1985).

32) T.A. DeGrand and C.E. DeTar, University of Colorado report, COLO-HEP-113 (1986).

33) B. Svetitsky and L.G. Yaffe, Nucl. Phys. B210, 423 (1982).

34) T.T Wu and C.N. Yang, in Properties of Matter under Unusual Conditions, eds. H. Mark and S. Fernbach (Interscience, New York, 1969).

35) Similar to the method used in G. Schierholz, J. Seixas and M. Teper, Phys. Lett. 157B, 209 (1985).

36) M. Teper, Phys. Lett. 171B, 81 (1986).

37) M. Göckeler, A.S. Kronfeld, M.L. Laursen, G. Schierholz and U.-J. Wiese, DESY report in preparation.

38) I. Barbour, N.-E. Behilil, P. Gibbs, M. Rafiq, K.J.M. Moriarty and G. Schierholz, DESY report 85-141 (1985), to be published in J. Comp. Phys.

β	V	$a^4\chi_t$	N_{tot}
2.2	6^4	$(7.45 \pm 1.17)\cdot 10^{-3}$	450
2.3	6^4	$(2.85 \pm 0.31)\cdot 10^{-3}$	250
2.3	10^4	$(3.06 \pm 0.11)\cdot 10^{-3}$	800
2.4	6^4	$(7.56 \pm 1.08)\cdot 10^{-4}$	200
2.4	8^4	$(10.12 \pm 0.61)\cdot 10^{-4}$	1600
2.4	10^4	$(11.14 \pm 0.21)\cdot 10^{-4}$	4000
2.5	6^4	$(2.78 \pm 0.46)\cdot 10^{-4}$	200
2.5	10^4	$(3.26 \pm 0.20)\cdot 10^{-4}$	800
2.5	12^4	$(3.58 \pm 0.13)\cdot 10^{-4}$	1400
2.6	10^4	$(1.08 \pm 0.15)\cdot 10^{-4}$	400
2.6	12^4	$(1.23 \pm 0.06)\cdot 10^{-4}$	1000

Table 1: Comparison of $a^4\chi_t$ from refs. [12,22].

Figure Captions

Fig. 1 The topological susceptibility $a^4\chi_t$.

Fig. 2 The ratio S/β as a function of the number of relaxation sweeps for 4 typical gauge field configurations in the confined phase.

Fig. 3 The action density S_x for a 3-dimensional cross section through the center of the "instanton". The integers plotted are $[100S_x/\beta]$. The dots correspond to zero.

Fig. 4 The eigenvalue density $\rho(\lambda)$ and the corresponding S/β for another 3 typical gauge field configurations. The arrow indicates where $\rho(\lambda)$ and Q where computed.

Fig. 5 The ratio S/β as a function of the number of relaxation sweeps for a selection of typical gauge field configurations in the deconfined phase.

Fig. 6 The colour electric and colour magnetic field strengths separately for configuration J [fig.5].

Fig. 7 The action density D_x for a 2-dimensional cross section through the center of the "monopole". The integers plotted are $[10D_x/\beta]$.

Fig. 8 Comparison of plateaus on $8^3\cdot4$, $10^3\cdot4$ and $12^3\cdot4$ lattices.

Fig. 9 The eigenvalue density $\rho(\lambda)$ of the 3-dimensional Dirac operator for (a) configuration H and (b) configuration J after 20 sweeps.

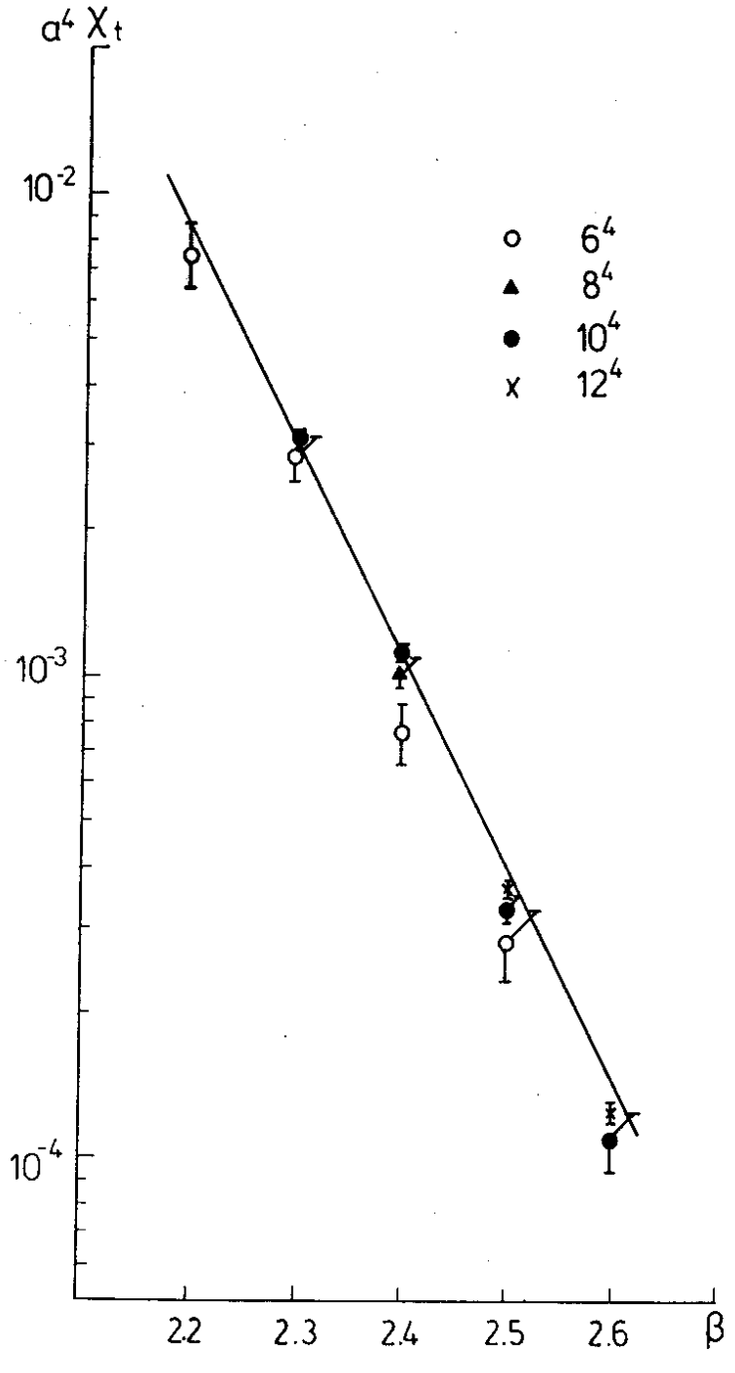

Fig.1

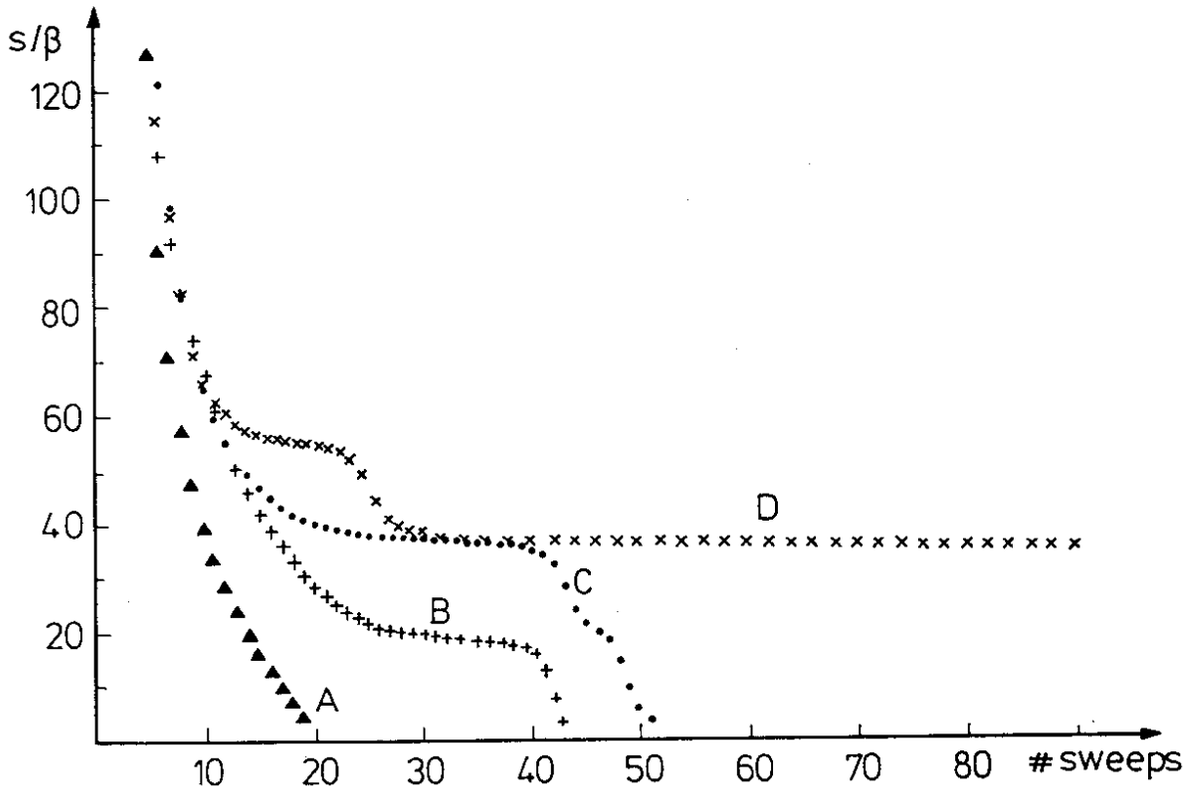

Fig. 2

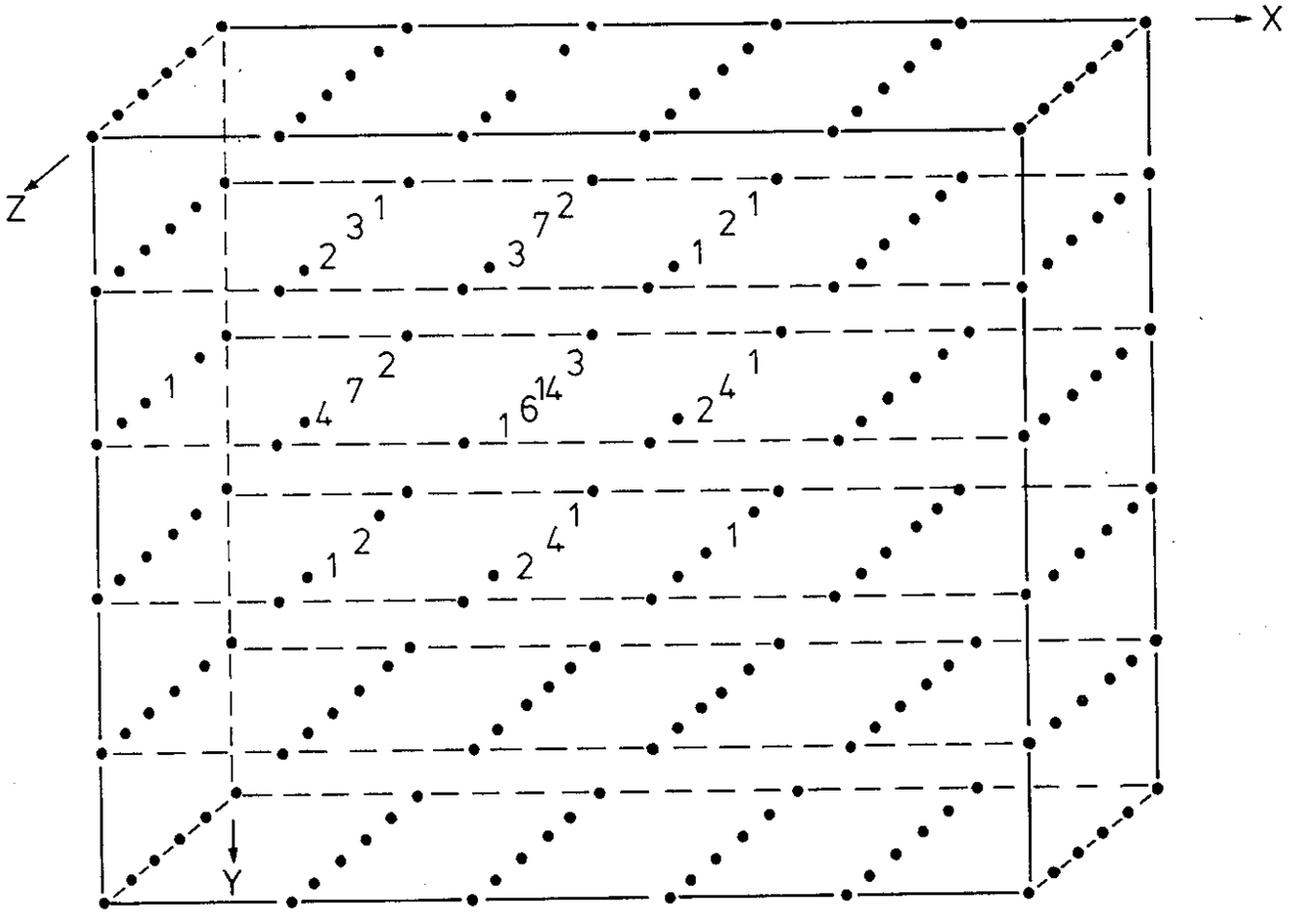

Fig. 3

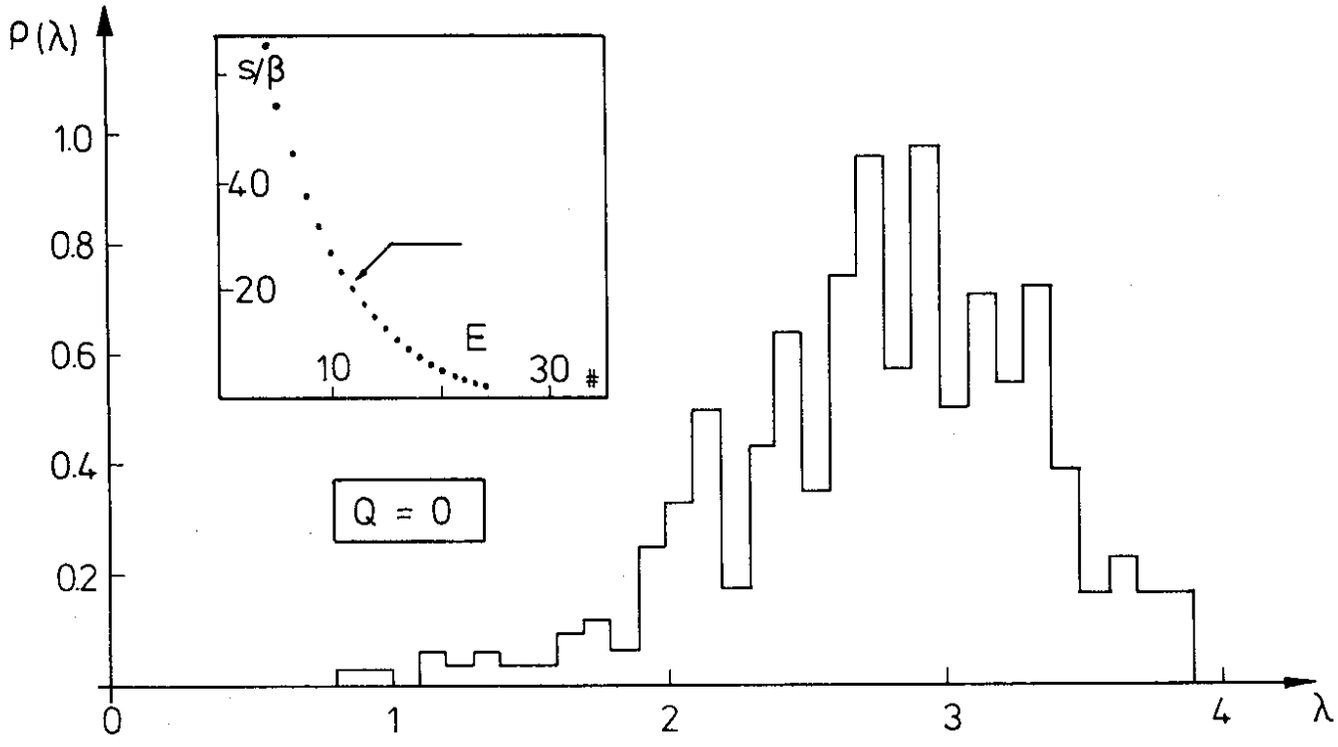
ρ(λ)
1.0
0.8
0.6
0.4
0.2
0
1
2
3
4
λ
s/β
40
20
10
30
#
E
Q = 0

Fig. 4a

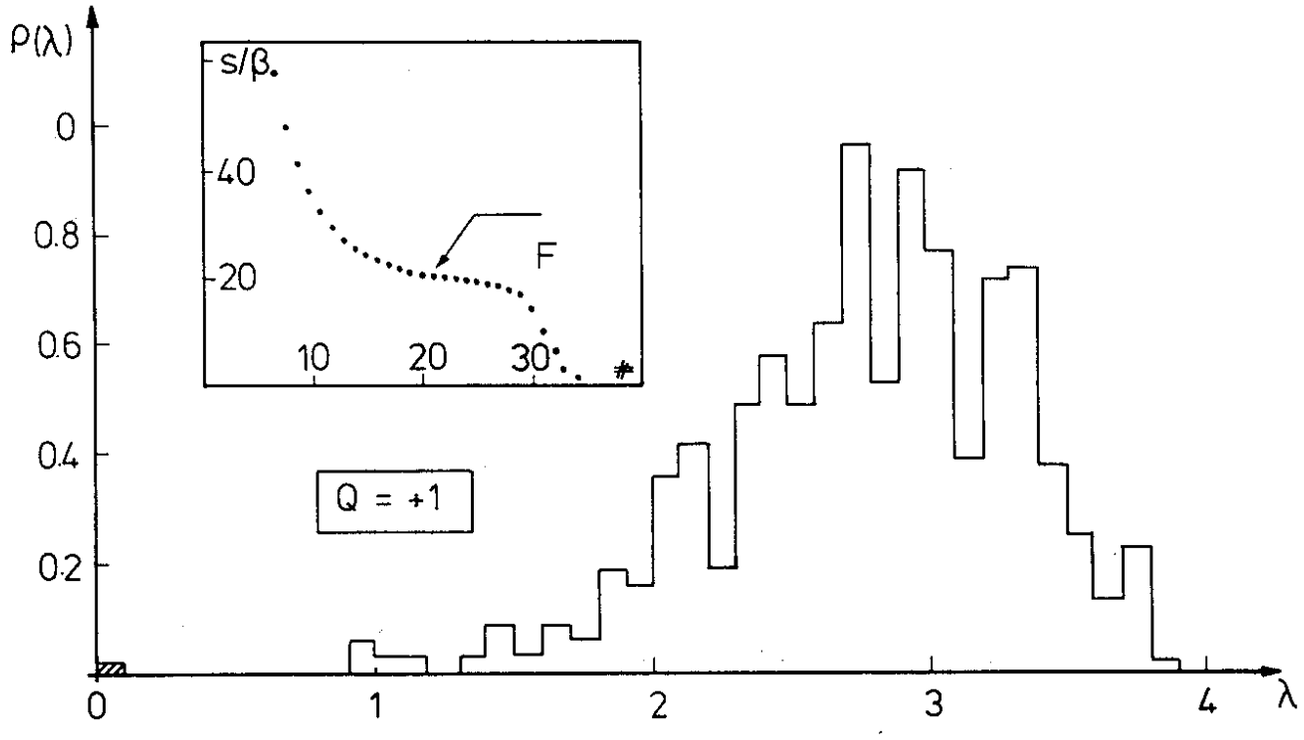
ρ(λ)
0
0.8
0.6
0.4
0.2
0
1
2
3
4
λ
s/β.
40
20
10
20
30
#
F
Q = +1

Fig. 4b

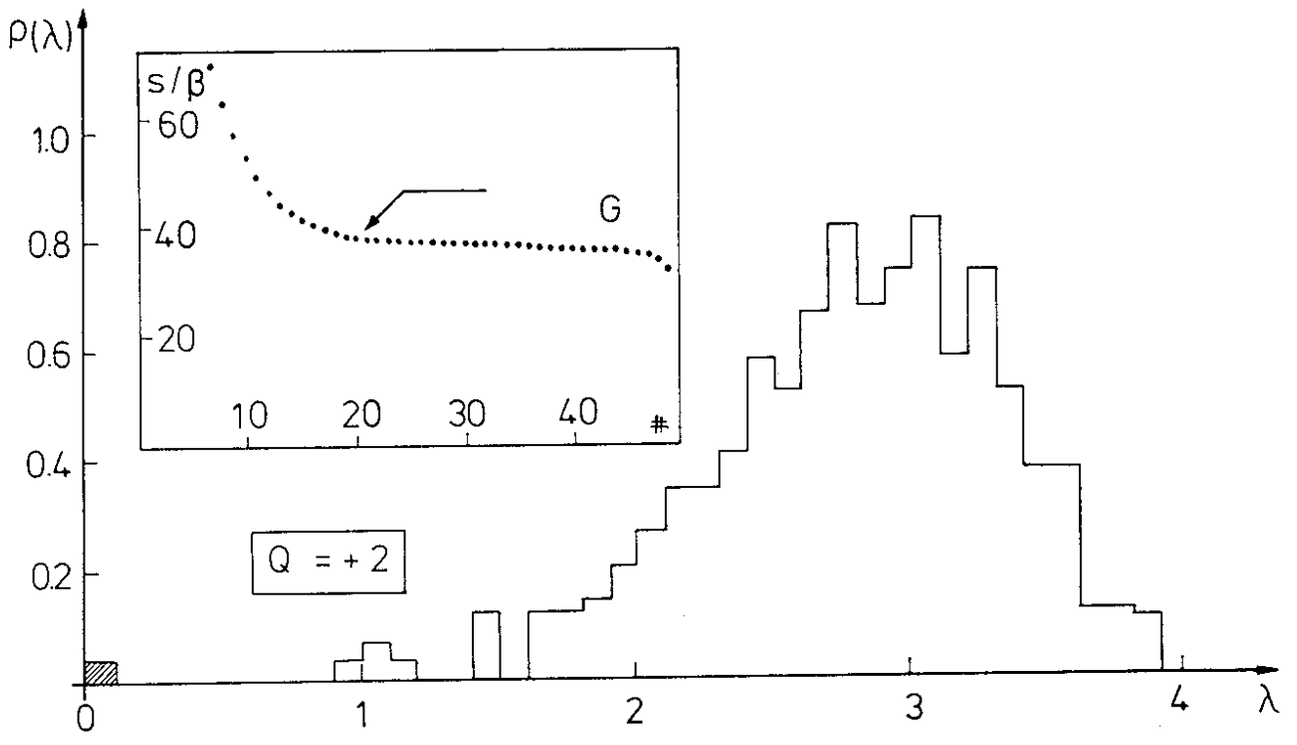
ρ(λ)
1.0
0.8
0.6
0.4
0.2
0
1
2
3
4
λ
s/β*
60
40
20
10
20
30
40
#
G
Q = + 2

Fig. 4 c

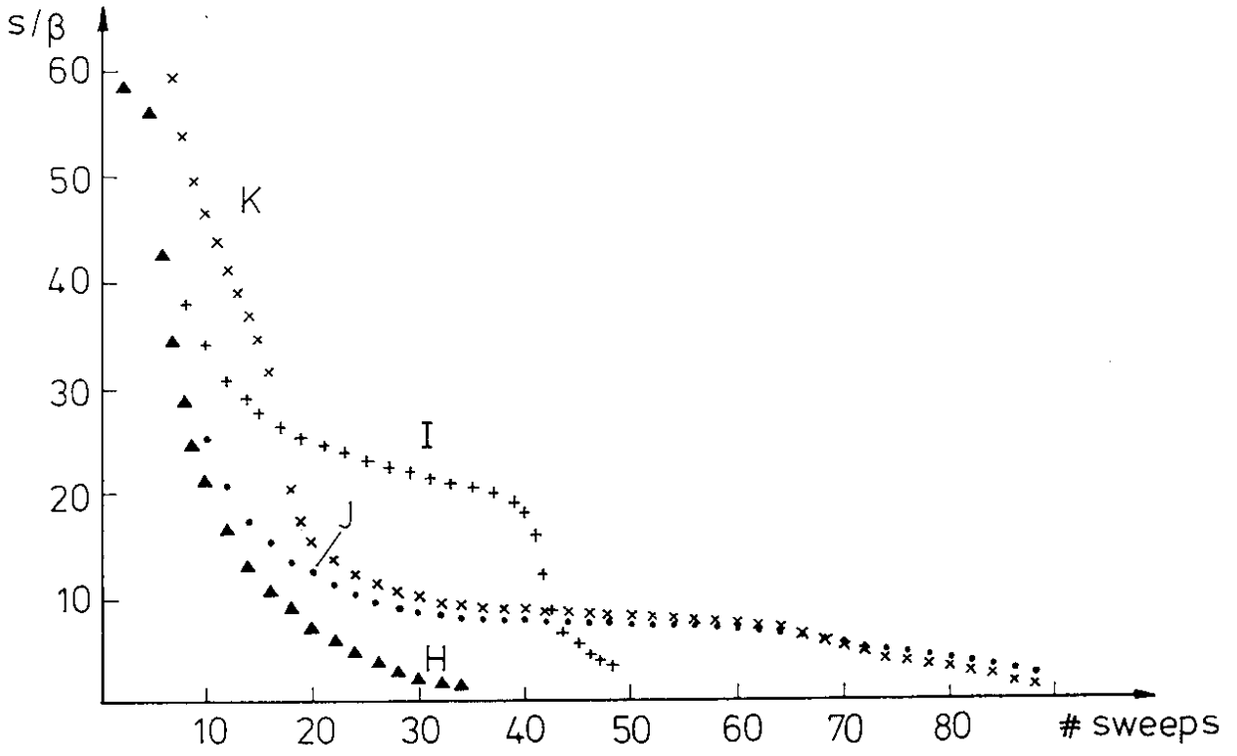
s/β
60
50
40
30
20
10
K
I
J
H
10
20
30
40
50
60
70
80
sweeps

Fig. 5

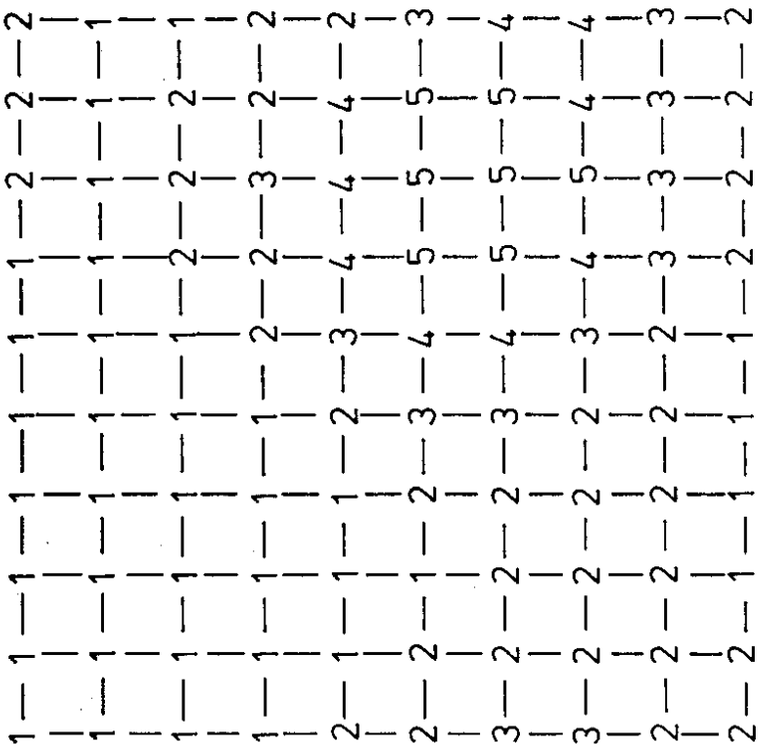

Fig. 7

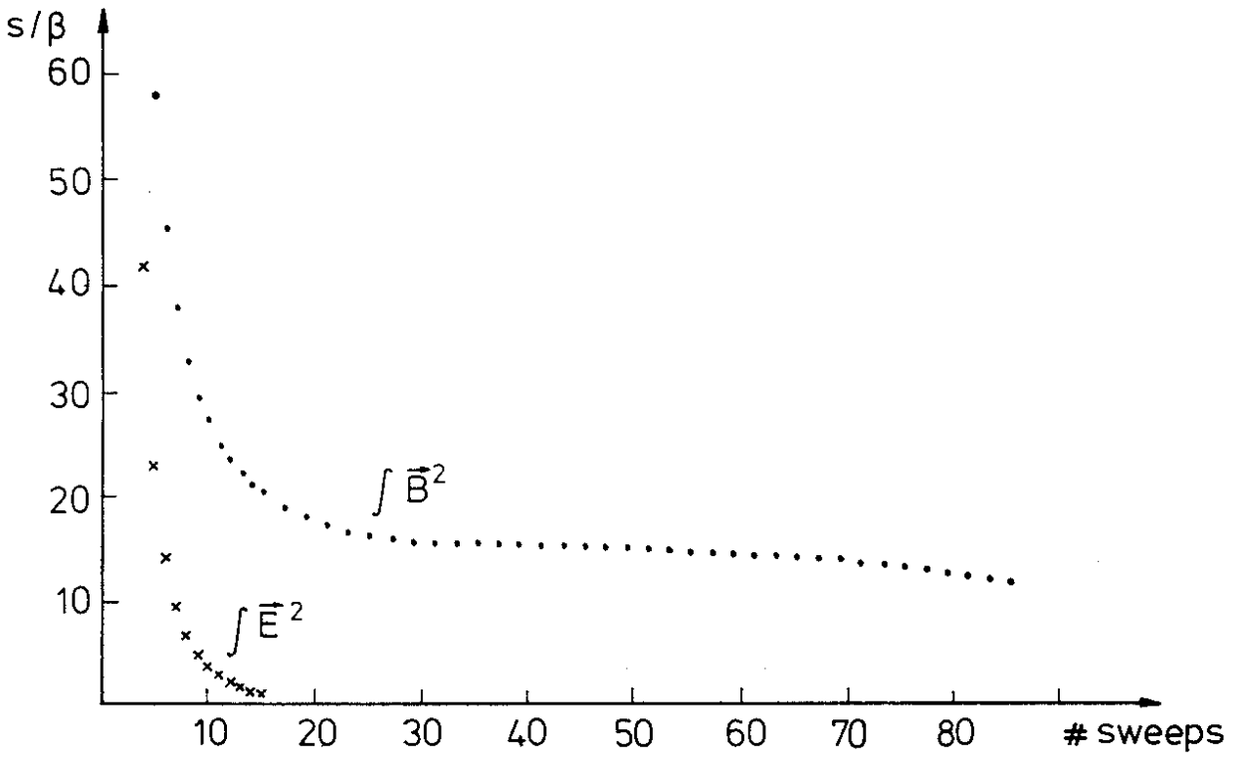
s/β
60
50
40
30
20
10
$\int \vec{B}^2$
$\int \vec{E}^2$
10
20
30
40
50
60
70
80
sweeps

Fig. 6

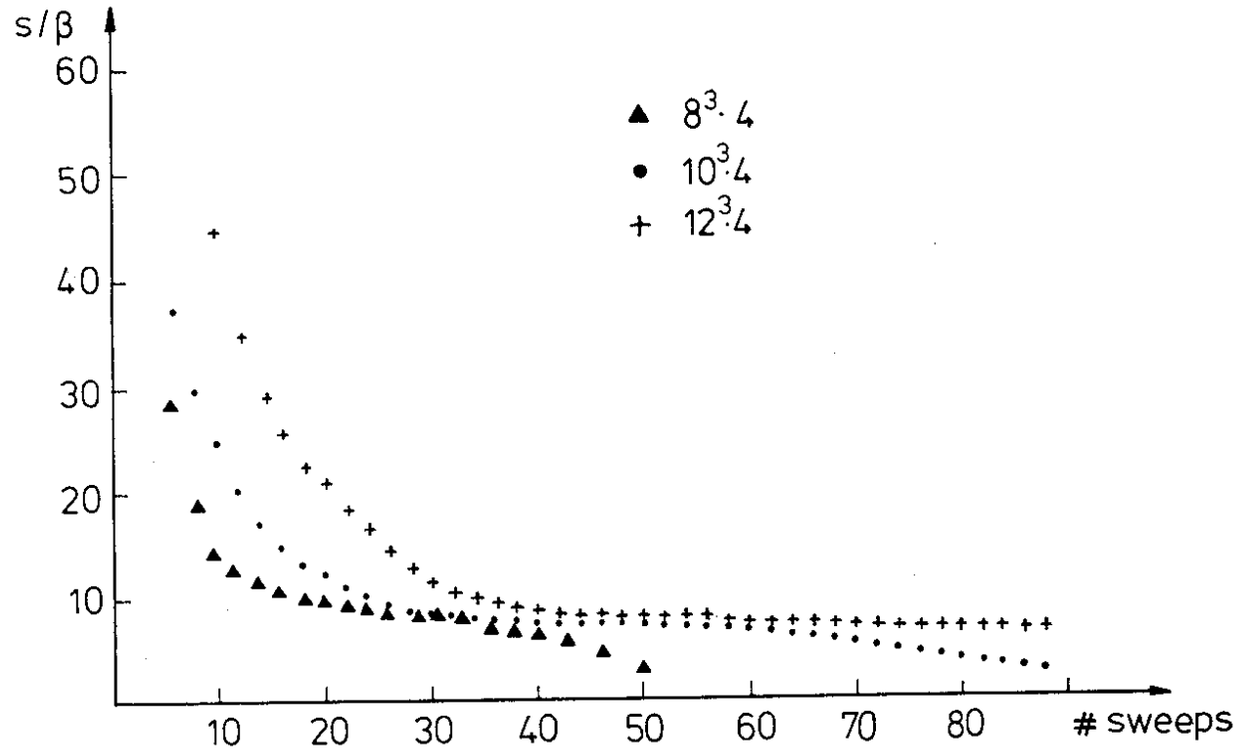
s/β
60
50
40
30
20
10
▲ $8^3 \cdot 4$
• $10^3 \cdot 4$
+ $12^3 \cdot 4$
10
20
30
40
50
60
70
80
sweeps

Fig. 8

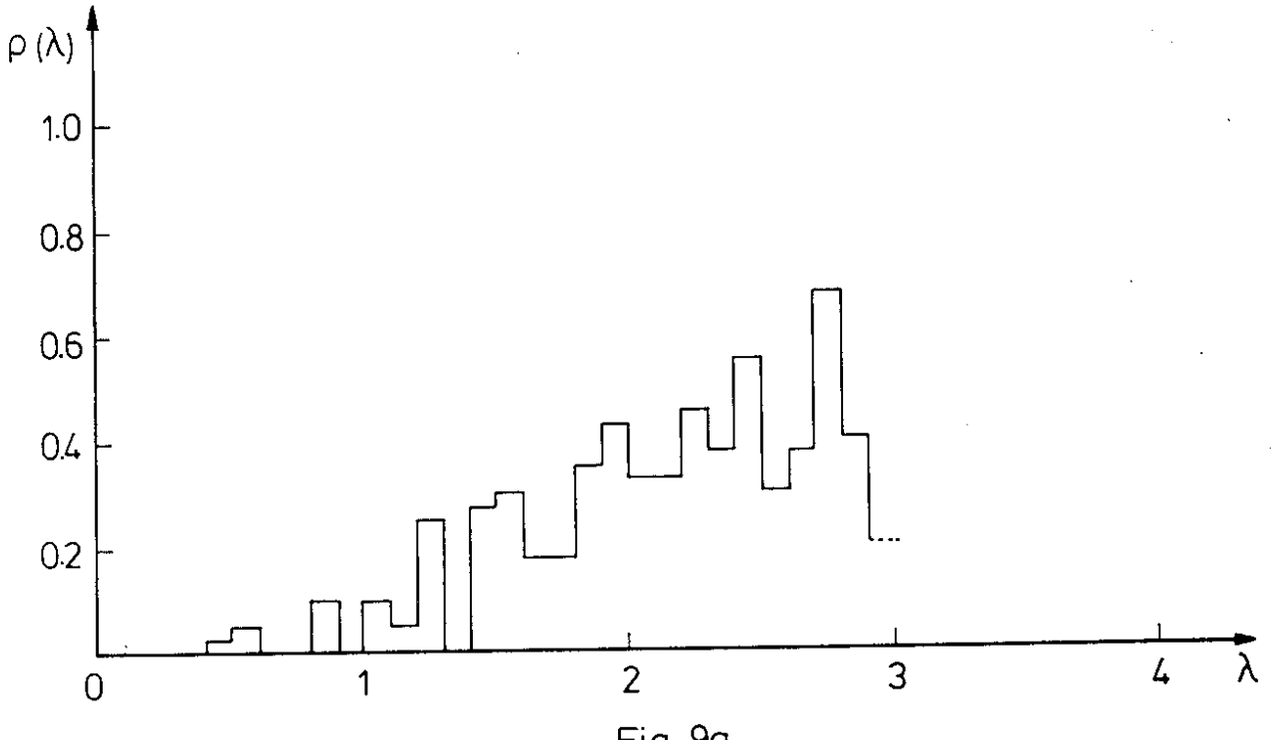
ρ (λ)
1.0
0.8
0.6
0.4
0.2
0
1
2
3
4
λ

Fig. 9a

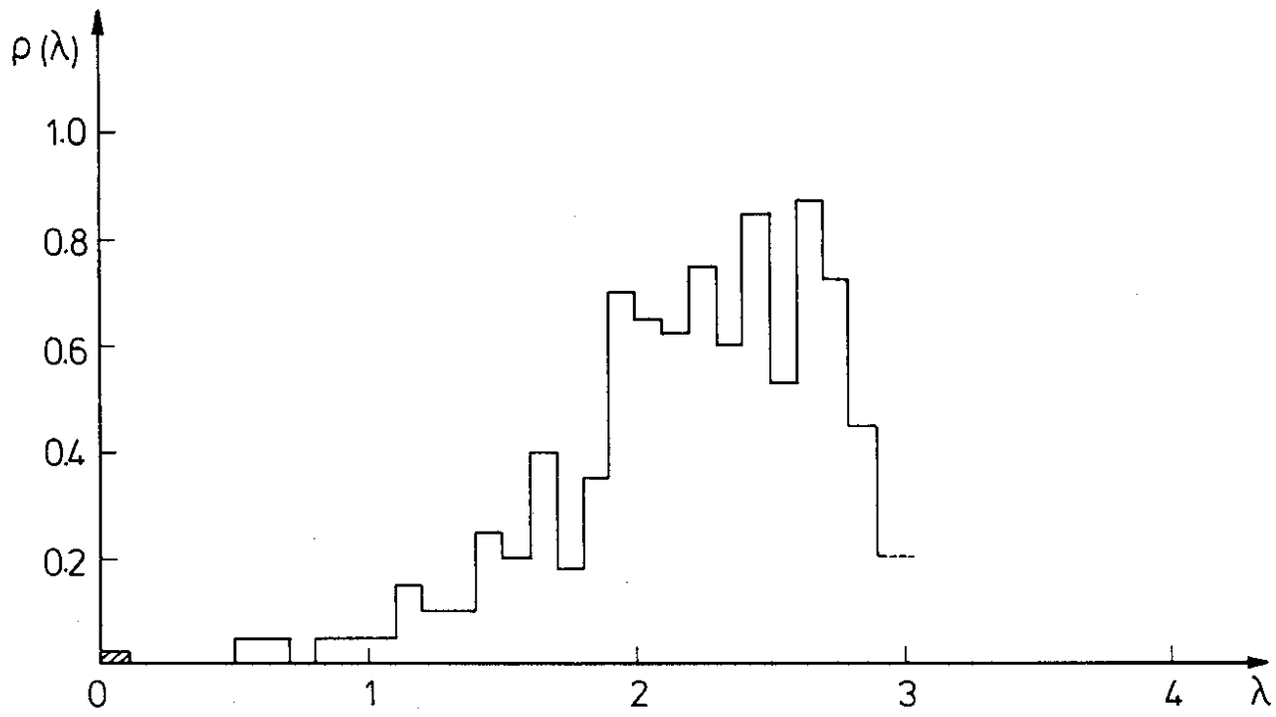

Fig. 9b